



SACRED HEART RESEARCH PUBLICATIONS

Journal of Functional Materials and Biomolecules

Journal homepage: www.shcpub.edu.in



ISSN: 2456-9429

SYNTHESIS OF LITHIUM COBALT OXIDE NANOPARTICLES VIA SOL-GEL METHOD

D. Daniel Lawrence^{1*}, E. Ashwini¹, S. Rahul¹, Amal George¹, Dominic Savio C¹

Received on 01 June 2023, accepted on 15 June 2023,
Published online on June 2023

Abstract

In the recent years, one of the most commercially wanted after energy storages are Lithium-ion batteries. Nanocrystalline Lithium cobalt oxide (LiCoO_2), Using the sol-gel method using an aqueous solution of metal nitrates, the most promising cathode materials for lithium-ion secondary batteries was synthesized. The chelating agents like oxalic acid and tartaric acid were assisted to get different size and morphology of particle. The optimized size may be achieved through sol-gel processing. The XRD, SEM, UV and FTIR characteristics were studied.

Keywords: Lithium-ion batteries, Oxalic acid and Tartaric acid.

1. Introduction

Since environmental and energy-related problems are closely related to technological advancement, they have emerged as the two main topics of concern in the twenty-first century. As a result, research into alternative energy sources is ongoing [1]. Due to the depletion of non-renewable resources and the steadily rising demand for energy, the energy economy, which relies primarily on fossil fuels, is currently in danger. Furthermore, one of the primary factors contributing to global warming, which is becoming a significant concern in international energy policy, is CO_2 emissions from the usage of fossil fuels [2, 3].

As a result, expenditures in the development of renewable energy sources are rising everywhere, with special focus on battery, solar, and wind power systems [4, 5]. As an alternate form of energy storage, batteries have various benefits. Currently, lithium-ion (Li-ion) batteries, fuel-cell technologies, and nickel metal hydride batteries are gradually replacing older battery technologies like lead-acid and nickel-cadmium batteries. Comparing Li-ion battery technology to other potential energy sources, it stands out as a pioneer and market leader [6].

The main reason for using this Li-ion battery technology is that lithium is the lightest and most electropositive metallic element, allowing for very high energy densities. Lithium-ion batteries have been discovered to be more maintenance-free, stable over 500 cycles, and available in a range of sizes than other battery technologies. Numerous parts of this technology are still being worked on, including lowering costs, extending cycle lifetime, and enhancing

safety [7, 8]. This technology is a real candidate to power the electric automobiles of the future because it is already widely used in electronics, has just entered the power tool sectors, and is now approaching the hybrid electric vehicle business [9, 10].

C. Deng et al., described that the two members of the family of orthosilicate, $\text{Li}_2\text{FeSiO}_4$ and $\text{Li}_2\text{MnSiO}_4$, are prepared by a citric acid assisted sol-gel method. As cathode materials for lithium-ion batteries, their structural, morphological and electrochemical characteristics are investigated and compared. Both cathode materials have nanoparticles with similar lattice parameters. $\text{Li}_2\text{FeSiO}_4$ has a maximum discharge capacity of 152.8 mA.hg^{-1} , and 98.3% of its maximum discharge capacity is retained after fifty cycles. However, the discharge capacity of $\text{Li}_2\text{MnSiO}_4$ fades rapidly and stabilized at about 70 mA.hg^{-1} after twenty cycles. The electrochemical impedance and differential capacity analysis indicate that $\text{Li}_2\text{MnSiO}_4$ has larger charge transfer impedance and higher electrochemical irreversibility than $\text{Li}_2\text{FeSiO}_4$, which makes its electrochemical behaviors seriously deteriorate and leads to difference between two silicate materials [11]. Jinli Yang et al., said that three-dimensional porous self-assembled $\text{LiFePO}_4/\text{graphene}$ (LFP/G) composite was successfully fabricated using a facile template-free sol-gel approach. Graphene nanosheets were incorporated into the porous hierarchical network homogeneously, which greatly enhances the electrical conductivity and efficient use of the LiFePO_4 (LFP), leading to an outstanding electrochemical performance of the hybrid cathodes. The obtained LFP/G composite has a reversible capacity of 146 mA.hg^{-1} at 17 mA.hg^{-1} after 100 cycles, which is more than 1.4 times higher than that of porous LFP (104 mA.hg^{-1}). Moreover, the porous LFP/G composite also exhibits a desirable tolerance to varied charge / discharge current densities [12].

2. Materials and Methods

2.1 Materials

All of the Chemicals used in this work were analytical grade reagents and used without further purification. Lithium nitrate [LiNO_3], Cobalt nitrate [$\text{Co}(\text{NO}_3)_2$], Oxalic acid

Corresponding Author: e-mail - daniel@shcpt.edu

¹ PG. and Research Department of Physics, Sacred Heart College (Autonomous), Tirupattur, Tamilnadu, India.

[C₂H₂O₄] and tartaric acid [C₄H₆O₆] were purchased from Merck company. Deionized water was used to prepare all solutions.

2.2 Synthesis of Lithium Cobalt Oxide Nanoparticles

Lithium nitrate and cobalt nitrate was used as reactants. 0.01 mol of lithium and 0.02 mol of cobalt nitrate mixture are dissolved in deionized water and done continuous stirring to get a homogenous solution. Chelating agents such as oxalic acid (0.03 mol) and tartaric acid (0.03 mol) were also added in the dissolved solution and continued 30 minutes of stirring. Then the stirring is continued with heat for another 3 hours to remove water molecules in the dissolved solution and finally the viscous gel is formed. After that the viscous gel is placed into the hot air oven for 3 hours to get dry sample. The obtained pink color dried sample is calcined at 550°C for 3 hours. Similar procedure is followed for other samples of LiCoO₂.

3. Results and Discussion

The samples of synthesized LiCoO₂ were characterized by powder XRD analysis, Scanning Electron Microscopy (SEM) morphological analysis, Fourier transform infrared (FTIR) spectral analysis and UV-Vis spectral analysis.

3.1 Powder X-Ray Diffraction Analysis.

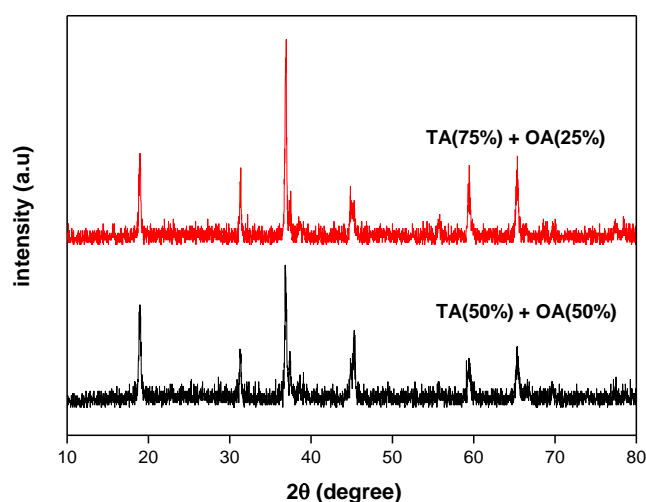


Figure 3.1 XRD patterns of synthesized LiCoO₂ calcined at 550°C, 3h using Oxalic Acid (OA) and Tartaric Acid (TA) as chelating agents

According to the spectrum shown in the aforementioned fig. 3.1, there is an increase in peak intensity when oxalic acid concentration as a chelating agent increases. The miller indices (hkl) values of main diffracted peaks are compared and matched with JCPDF file #77-1370. The observed 2θ values are 18.96, 36.89, 44.91, 59.46, and 65.35 are associated with (003), (101), (104), (109), and (018) planes [13, 14]. From the analysis it shows that rhombohedral structures are observed. The crystallite size “d” is calculated using the Debye Sherrer formulae

$$d = 0.9\lambda / \beta \cos\theta \text{ nm}$$

Table 3.1 Average crystallite size of LiCoO₂ synthesized with different chelating agents

Sample	Chelating Agents	Average crystallite size in nm
LiCoO ₂	Tartaric acid (75%) + Oxalic acid (25%)	23
	Tartaric acid (50%) + Oxalic acid (50%)	22

The average crystallite size of LiCoO₂ using tartaric acid and oxalic acid as chelating agents is 23 nm and 22 nm (Table 5.1). From the table it shows that average crystallite size decreases as the concentration of chelating agent oxalic acid increases and their average crystallite size is found to be 23 & 22 nm respectively [15-18].

Table 3.2 Lattice constants, c/a ratio, and I (003) / (101) of LiCoO₂ synthesized using different chelating agents

Sample	Chelating Agents	a (Å)	c (Å)	c/a	I (003) / (101)
LiCoO ₂	Tartaric acid (75%) + Oxalic acid (25%)	2.815	14.050	4.991	1.2
	Tartaric acid (50%) + Oxalic acid (50%)	2.815	14.050	4.991	1.49

When the concentration of oxalic acid as a chelating agent increases, the intensity ratio also tends to increase gradually as 1.2, and 1.49 respectively. It clearly reveals that the electrochemical performance of LiCoO₂ cathode material could be lesser for tartaric acid than oxalic acid as chelating agents.

The performance of the cathode in lithium batteries is significantly influenced by the material's particle size and crystalline phase. Smaller size distribution resulted in better cycle stability [19]. Thus from the XRD pattern it concludes that lesser crystalline size of synthesized LiCoO₂ with oxalic acid as a chelating agent have better electrochemical performance than synthesized LiCoO₂ with tartaric acid as a chelating agent [20-22].

3.2 MORPHOLOGICAL STUDIES

The morphology of LiCoO₂ calcined at 550°C for 3hrs are analyzed with SEM images.

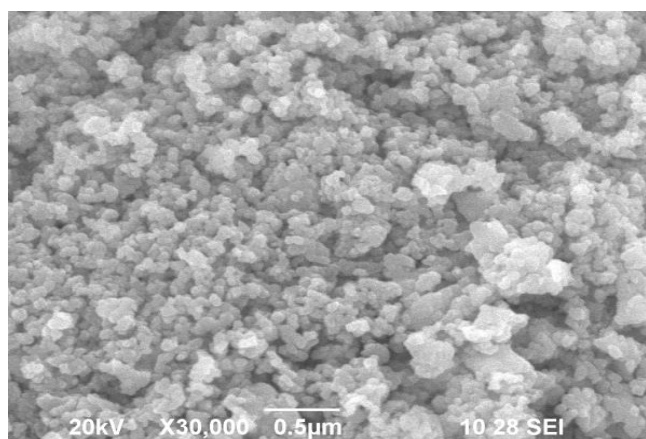


Figure 5.2 SEM image of LiCoO₂ with tartaric acid (75%) and oxalic acid (25%)

SEM image of LiCoO₂ shows sphere like structure particles. Thus the average particle size is 135 nm when measured under 0.5 µm.

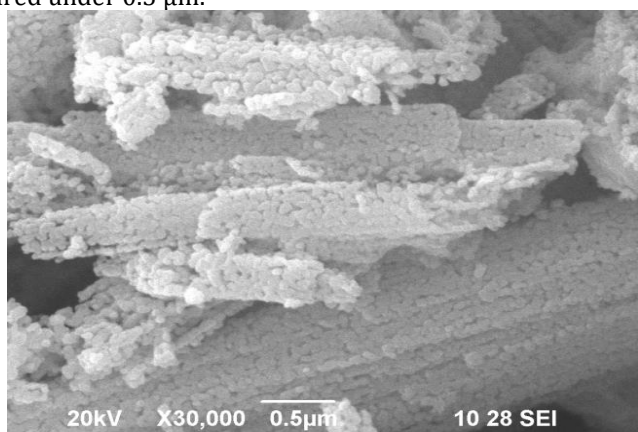


Figure 5.3 SEM image of LiCoO₂ with tartaric acid (50%) and oxalic acid (50%)

The SEM image reveals rod like structure where some rod structures are not completely formed. The average particle size is 210 nm, measured under 0.5 µm.

5.3 FTIR STUDIES

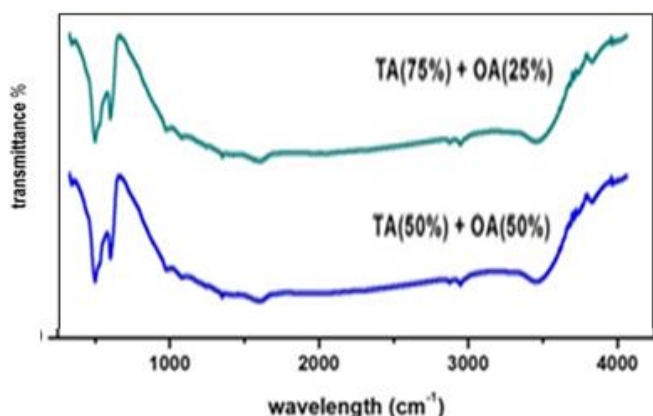


Figure 5.4 FTIR spectra of LiCoO₂ prepared by sol-gel method using oxalic acid and tartaric acid as chelating agents

Through the FTIR spectrum, the sample's chemical bonding vibrations are recorded. Fig 3.3 shows FTIR spectra of LiCoO₂ prepared by sol-gel method using oxalic acid and tartaric acid as chelating agents. The spectra were recorded from 400 - 4000 cm⁻¹ frequency. Functional group analysis predicts that there are two IR active bands. The FTIR bands of LiCoO₂ are 565, 663, 1397, 2928 and 3398 cm⁻¹ [23-24]. The peaks of the metal oxide are confirmed by the bands seen at 565 and 663 cm⁻¹ frequency [25]. The higher frequency band is located at 1397 cm⁻¹ frequency attributed to asymmetric modes of CoO₂. The frequency band 2928 cm⁻¹ is attributed to -CH₃ stretching is attributed to organic impurity present in the sample [26]. The band 3398 cm⁻¹ is -OH stretching vibration [27].

5.4 UV-Vis Spectral analysis

For LiCoO₂, the optical absorption spectrum is shown. The range of the absorption spectrum is 200–800 nm. From the absorption spectrum the conductivity band gap energy is calculated. The energy band gap is calculated using the formula

$$E_g = hc/\lambda \text{ (eV)}$$

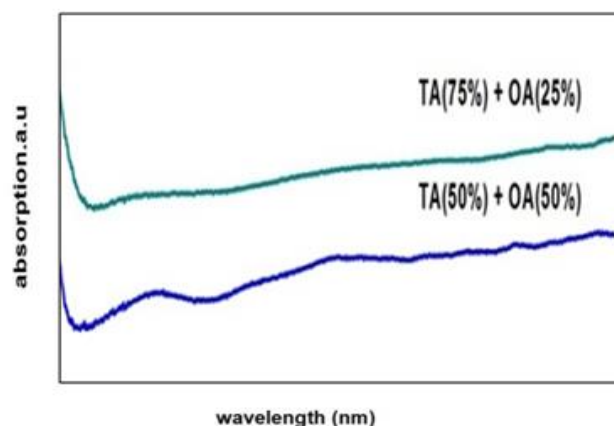


Figure 5.5 UV-Vis spectrum of LiCoO₂ calcined at 550°C, 3h using oxalic acid and tartaric acid as chelating agents

The Figure 5.8 shows the UV-Vis spectrum of LiCoO₂ with oxalic acid and tartaric acid as chelating agents. The absorption spectrum range and its conductivity band gap energy is tabulated below

Table 5.1 Absorption range and conductivity band gap energy of LiCoO₂ synthesized with different chelating agents

Sample	Chelating Agents	Absorption range (nm)	Band gap energy (eV)
LiCoO ₂	Tartaric acid (75%) + Oxalic acid (25%)	209	5.9
	Tartaric acid (50%) + Oxalic acid (50%)	213	5.8

The band gap energy of LiCoO₂ using tartaric acid and oxalic acid as chelating agents is 5.9 eV and 5.8 eV (Table 5.3) [28-29]. From the table it shows that band gap energy decreases as the concentration of chelating agent oxalic acid increases and their value is found to be 5.9 eV, and 5.8 eV respectively [30].

Conclusion

The sol-gel process has been used to successfully synthesize of LiCoO₂ nanocrystallines. Oxalic acid and tartaric acid are used as chelating agents, and their concentrations are changed to create different samples of LiCoO₂. Using the Debye-Scherrer formula, the LiCoO₂ nanocrystallines' dimensions were determined. Rhombohedra structure is observed from the XRD pattern. The XRD pattern concludes that lesser crystalline size of synthesized LiCoO₂ with oxalic acid as a chelating agent have better electrochemical performance than synthesized LiCoO₂ with tartaric acid as a chelating agent. The SEM images shows sphere like structure formation with little agglomeration in it. From the SEM images the average crystallite size is found 100 to 250 nm. The FTIR bands of LiCoO₂ are observed and it is also matched with the literature. The band gap energy for the different samples is found.

REFERENCES

- [1] Scrosati, B. and Jurgen Garche, Journal of Power Sources, 195 (2010) 2419-2430.
- [2] M. Armand, Journal of materials issue and challenges facing rechargeable lithium batteries, Nature, 414 (2001) 359-367.
- [3] G. N. Lewis, Journal of American Chemical Society, 192 (1913) 1126-1127.
- [4] C. Denga, Materials Chemistry and Physics 120 (2010) 14-17.
- [5] M. Bakierskaa, Journal of Power Sources 10 (2010) 10-28.
- [6] M. S. Whittingham, Electrical Energy Storage and Intercalation Chemistry, Science, 192 (1976) 1126-1127.
- [7] M. Stanley Whittingham, Journal of Chemical Science 104 (2004) 4271-4403.
- [8] M. Wakihara, Journal of Material Science and Engineering R, 33 (2001) 109-134.
- [9] J. L. Tirado Journal Material Science Engineering R, 40 (2003) 103-136.
- [10] E. V. Makhonina, Journal of Russian Chemical Reviews, 73 (2004) 991-1001.
- [11] S. T. Aruna, A. S. Mukasyan, Curr. Opin. Solid State Mater. Sci. 12 (2008) 44.
- [12] Z. S. Peng, Journal of Power Sources 72 (1998) 215-220.
- [13] Yuanxiang Gu, Journal of Physical Chemistry B, 109 (2001) 17901-17906.
- [14] Tetsuya Kawamura, Journal of Power Sources 146 (2005) 27-32.
- [15] Masashi Okubo, Journal of American chemical society 129 (2007) 7444-7452.
- [16] Forest T. Quinlan Indian Engineering Chemistry 43 (2004) 2468-2477.
- [17] Kiyoshi Kanamura, Journal of solid state ionics 151 (2002) 151-157.
- [18] Sina Soltanmohammad, Journal of nanomaterials 91 (2010) 1-8.
- [19] Hailong Chen A, Journal of Electrochemistry Communications 4 (2002) 488-491.
- [20] K. Suryakala, Journal of Electrochemistry Communications 4 (2006) 478-491.
- [21] Shuxin Liu, Journal of Power Sources 147 (2007) 17-32.
- [22] Yand-Kook Sun, Indian Engineering Chemistry 36 (1997) 4839-4846.
- [23] Hai-Tao Xu, Journal of American Chemical Society 10 (2011) 4471-4475.
- [24] Naiteng Wu, Journal of ACS Applied Materials & Interfaces 15 (2012) 23-42.
- [25] Katsuya Teshima, Journal of American Chemical Society 10 (2010) 4471-4475.
- [26] M. Bakierskaa, Journal of Power Sources 10 (2010) 10-28.
- [27] Jinli Yanga, Journal of Power Sources 208 (2012) 340-344.
- [28] Linmin Wu, Journal of Power Sources 10 (2010) 10-28.
- [29] R. Santhanam, Journal of Power Sources 195 (2010) 5442-545.
- [30] H. Heli, Journal of Applied Electrochemisrty 42 (2012) 279-289.